

E. Demey¹, S. Liuu¹, E. Durighello¹, M. Colombat², G. Grateau², J. Vinh¹

¹SMBP CNRS USR 3149, ESPCI PARISTECH, ²Service d'anatomie pathologique, AP-HP Hopital Tenon, Paris, France

Introduction. Amyloidosis is a disease where specific proteins aggregate in tissues. Different classes of amyloidosis have been reported and their diagnostic relies on the identification of the associated proteins: up to 29 proteins families can be targeted using histochemical approaches. However they can be inconclusive on certain cases, leading to a lack of information about the underlying etiology. Recent reports have shown that subtyping could be feasible combining laser capture microdissection and mass spectrometry (1). For bottom-up proteomics it is clear that one of the key factors is the completion of enzymatic proteolysis. Ultrasonic treatment could help for this step (2). We have tried to extend the use of ultrasonic treatment to raw biopsy samples in order to avoid the tedious step of LCM and to get closer to the clinical routine application for amyloidosis subtyping.

Methods. Biopsy sample were taken from diseased and control patients. Tissues were immobilized with paraformaldehyde (Bouin or AFA). Tissues and reference proteins were directly digested using an ultrasonic probe. Proteolytic peptide mixtures were analyzed by nanoLC-MS/MS (LTQ-FT Ultra, ThermoFisher) after LC optimization (U3000 Dionex).

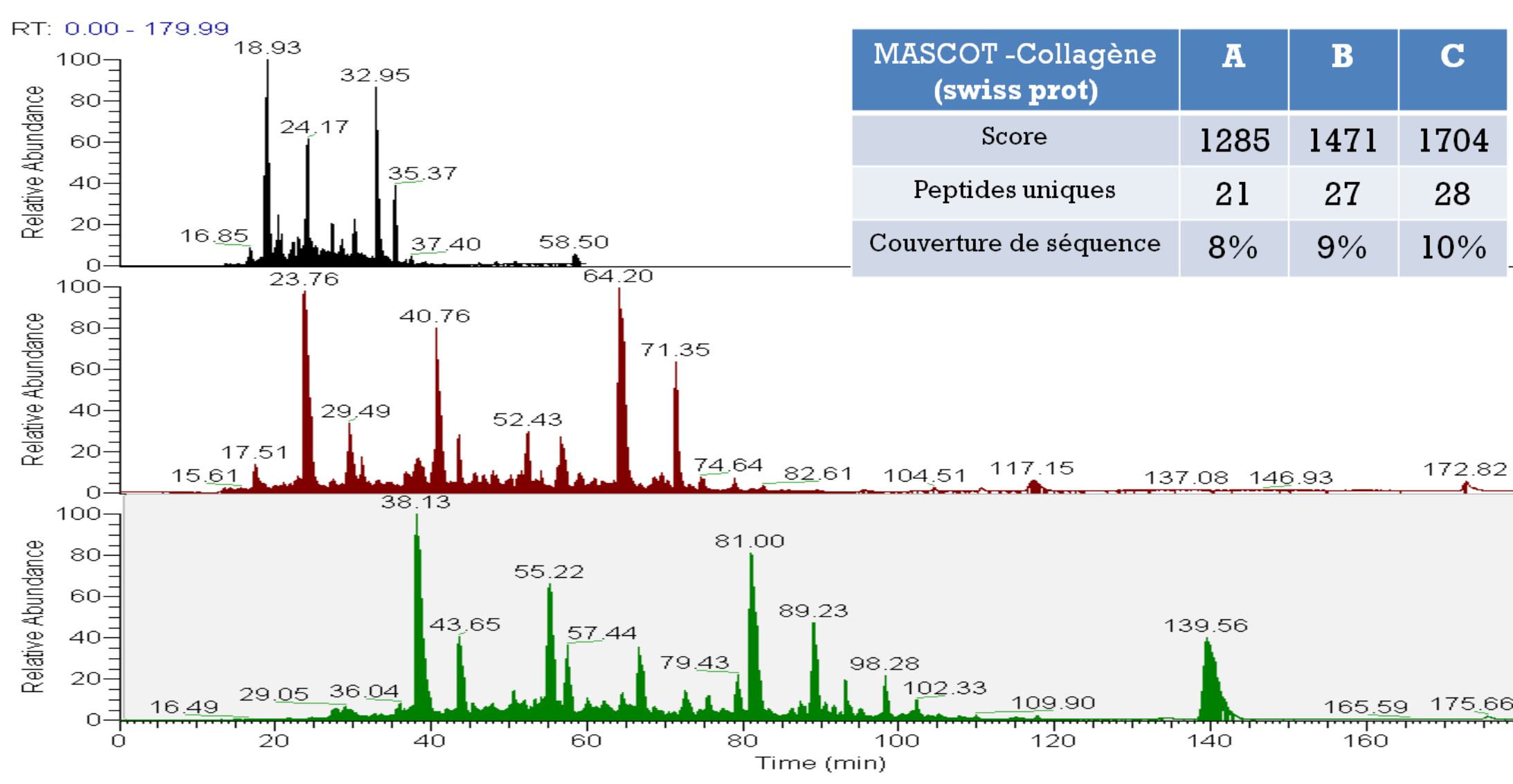


Figure 1: LC optimization on lung biopsy sample

- *nano C18 Acclaim pepMap100 (Dionex) Viper 75µm i.d.x15cm length column, gradient 2% to 40%B in 170 min, buffer A: H2O/AcN/AF 98:2:0.1 (v/v/v)/ buffer B: H2O/AcN/AF 10:90:0.1 (v/v/v)
- *Advion nano ESI source, acquisition method: 1 FTMS (Res100000) + top 7 CID LIT MS/MS
- *database search using Proteome Discoverer 1.3.0.339 combining Mascot 2.3 and Sequest on UniProt-SwissProt 2011_07 and home made SwissProt/Trembl database containing amyloidosis proteins, 5ppm MS, 0.5Da MS/MS, up to 2 miscleavages, full tryptic peptides, Ox (M) and CAM (C) as partial modifications.
- *only consensus proteins identified in triplicate with both search engine with a FDR<1% are kept
- *digestion with porcine trypsin (Promega Gold), after reduction (TCEP 2.5mM), alkylation (iodoacetamide 10mM), in ammonium bicarbonate 50mM pH 8.4 using an ultrasonic probe MicroSon XL on a wet ice bath
- *tissues slices of 10µm, volume extrapolated using surfaces of slices as measured by anatomopathology
- *injected sample were filtered on Proxeon stage tips and reconstituted in the same volume, roughly 0.15 mm3 were injected for each LC (except for the comparison with Laser Capture Microdissection sample where 0.0055 mm3 were injected, 0.3 equivalent slice).

Accession	Amyloidosis	Description
P02743	non specif	>sp P02743 SAMP_HUMAN Serum amyloid P-component
P02649	non specif	>sp P02649 APOE_HUMAN Apolipoprotein E
P02766	ATTR	>sp P02766 TTHY_HUMAN Transthyretin
P04279	ASeml	>sp P04279 SEMGL_HUMAN Semenogelin-1
Q9UKY0	APrPsc	>sp Q9UKY0 PRND_HUMAN Prion-like protein doppel
Q865H4	APrPsc	>sp Q865H4 PRND_HUMAN Putative testis-specific prion protein
P04156	APrPsc	>sp P04156 PRIO_HUMAN Major prion protein
P01236	APrPc	>sp P01236 PRL_HUMAN Prolactin
Q08431	AMed	>sp Q08431 MFGM_HUMAN Lactadherin
P61626	Alys	>sp P61626 LYSC_HUMAN Lysozyme C
P0C606	AIL	>sp P0C606 LAC3_HUMAN Ig lambda-3 chain C regions
P0C605	AIL	>sp P0C605 LAC2_HUMAN Ig lambda-2 chain C regions
P0C604	AIL	>sp P0C604 LAC1_HUMAN Ig lambda-1 chain C regions
P0CF74	AIL	>sp P0CF74 LAC6_HUMAN Ig lambda-6 chain C region
A0M8Q6	AIL	>sp A0M8Q6 LAC7_HUMAN Ig lambda-7 chain C region
P01834	Alk	>sp P01834 IGKC_HUMAN Ig kappa chain C region
Q14960	ALect2	>sp Q14960 LECT2_HUMAN Leukocyte cell-derived chemotaxin-2
P02788	Alac	>sp P02788 TRFL_HUMAN Lactotransferrin
Q15582	Aker	>sp Q15582 BGH3_HUMAN Transforming growth factor-beta-induced protein ig-h3
P01308	AIns	>sp P01308 INS_HUMAN Insulin
P10997	AIAPP	>sp P10997 IAPP_HUMAN Islet amyloid polypeptide
P01871	AHm	>sp P01871 IGHM_HUMAN Ig mu chain C region
P01857	AHlg	>sp P01857 IGHL1_HUMAN Ig gamma-1 chain C region
P06396	AGel	>sp P06396-2 GELS_HUMAN Isoform 2 of Gelsolin
P06396	AGel	>sp P06396 GELS_HUMAN Gelsolin
P02671	AFib	>sp P02671 FIBA_HUMAN Fibrinogen alpha chain
P01034	ACys	>sp P01034 CTC_HUMAN Cystatin-C
P01258	ACal	>sp P01258 CALC_HUMAN Calcitonin
P05067	ABeta	>sp P05067 A4_HUMAN Amyloid beta A4 protein
P61769	AB2M	>sp P61769 B2MG_HUMAN Beta-2-microglobulin
P06727	AApoAIV	>sp P06727 APOA4_HUMAN Apolipoprotein A-IV
P02652	AApoAII	>sp P02652 APOA2_HUMAN Apolipoprotein A-II
Q8NWC5	AApoA1	>sp Q8NWC5 A1BIP_HUMAN Isoform 2 of Apolipoprotein A-I-binding protein
P02647	AApoA1	>sp P02647 APOA1_HUMAN Apolipoprotein A-I
P01160	AANF	>sp P01160 ANF_HUMAN Natriuretic peptides A
P02735	AA	>sp P02735 SAA_HUMAN Serum amyloid A protein

Table 1: List of proteins associated to amyloidosis that were considered in this study.

Data interpretation. It is a non targeted approach. Only one isoform is listed for each group, and only proteins that are validated and annotated in SwissProt were considered. Abundance of the protein were evaluated according to (5) taking into account the area of the three most intense peptides. Unidentified species were given the global minimum intensity that could be calculated in our experiments. Only biopsies exhibiting a relative abundance >1% and containing Apolipoprotein E and Serum amyloid P component (common to all amyloid deposits) were considered as potential amyloid candidate. Finally amyloidosis were classified according to the relative intensity of protein listed in Table 1.

Results. Application of ultrasonic tryptic treatment on fixed raw tissues allowed us to perform subtyping of amyloidosis. The results were independantly confirmed by immunohistopathology. Using the whole series of antibodies for amyloidosis diagnostic. We have selected some examples from different tissueand pathologies to illustrate our results. The results are visualized with sector diagrams representing the relative intensities of amyloid proteins.

Kidney Results.

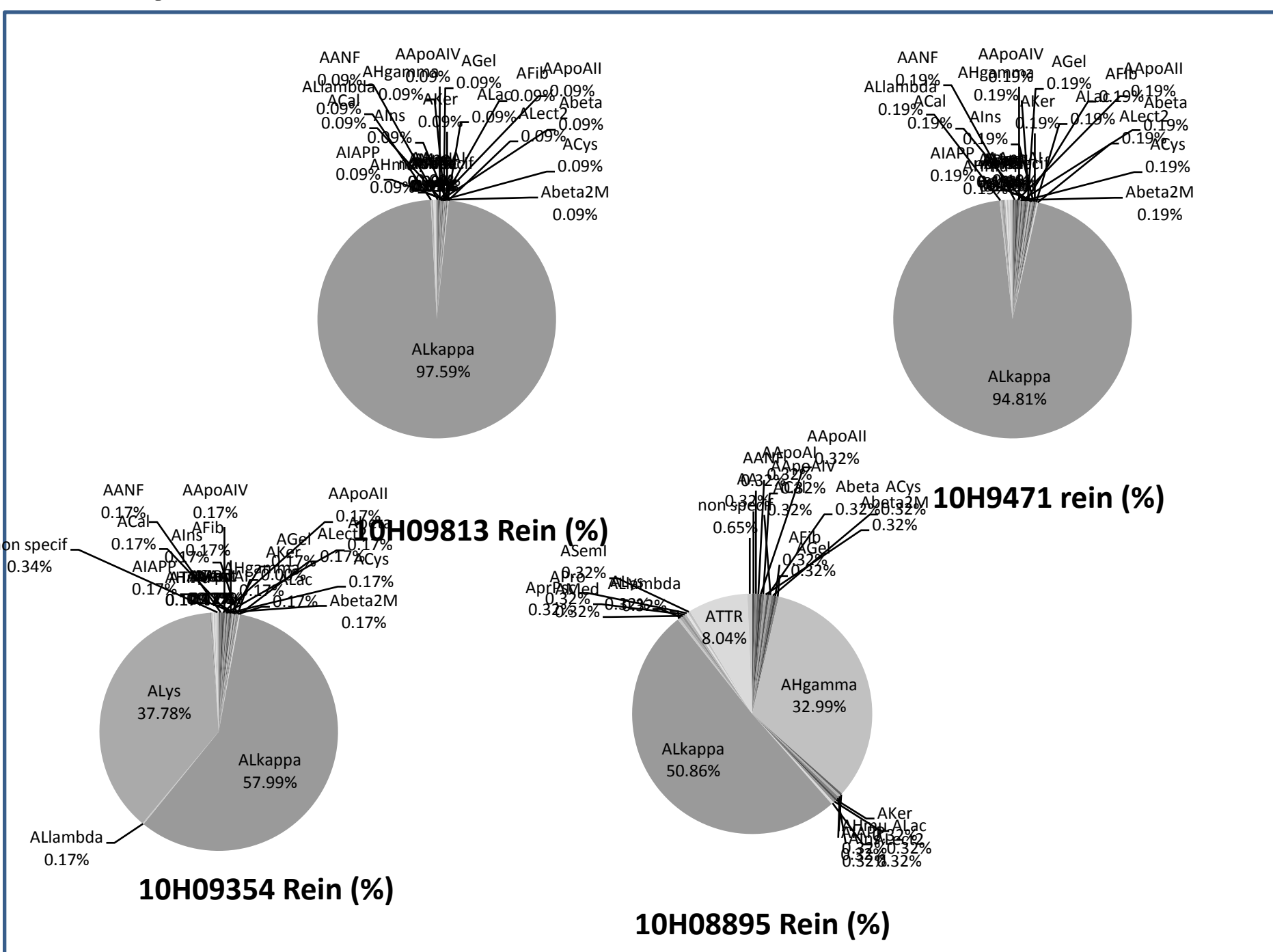


Figure 3: Biopsies of negative controls.

No pure negative controls could be assayed because biopsies come always from patients and are aimed to identify a pathology. Non amyloid diseased kidney does not present SAMP and ApoE (fibrils biomarkers), even if amyloidogen protein could be detected (Igκ and γ). Their presence could be explained by inflammatory phenomenon or tissue damage (eg. minor glomerular lesions). The controls are non amyloid pathologies. As shown in this example when amyloid deposits represents more than 80% of the tissue the diagnostic and the classification are clear (Figure 4 A). When the percentage goes below 50%, amyloid diagnostic is clear but classification is not robust enough (Figures 4B & 5A) even if the amyloid type is correct: here we analyzed a raw biopsy without focalising on amyloid fibrils and without slicing. On the opposite LCM treatment on the same sample could offer preparation above 95% where the classification is unambiguous (Figure 5B).

Figure 2: Anatomopathology studies of kidney biopsy for AAL with (A) Hemalun Eosin (HE), (B) Congo red, (C) immunostaining AL

Less than 50% of the tissue were marked for amyloidosis AAL (see C)

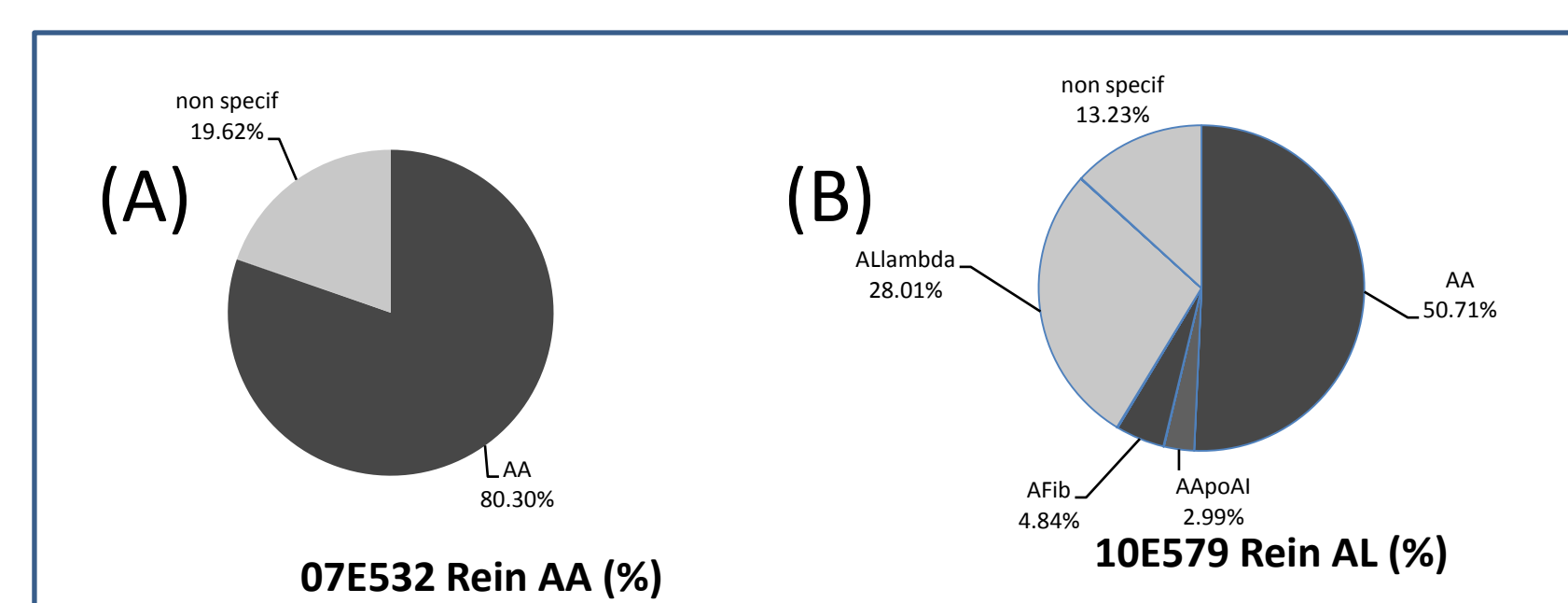
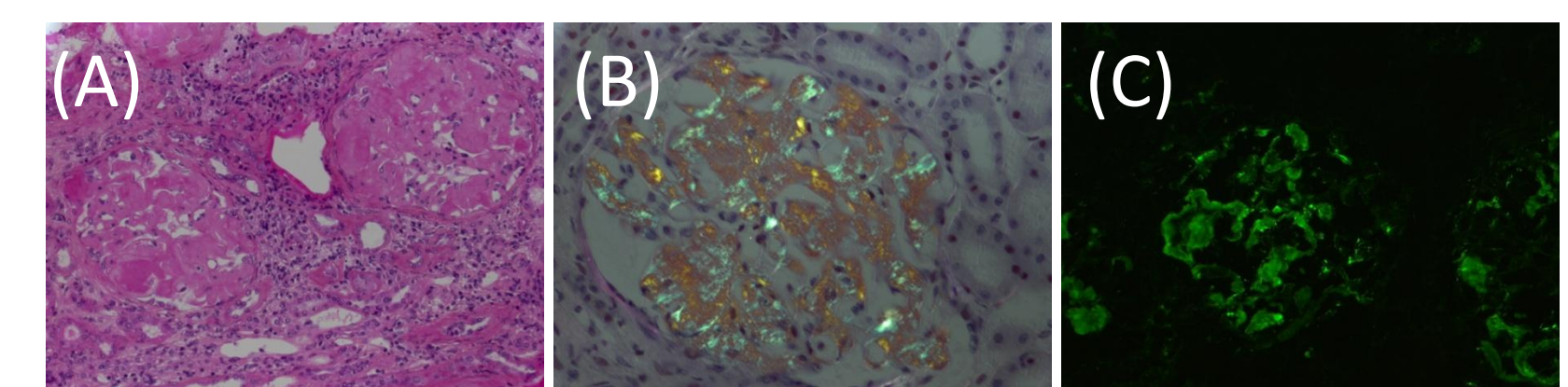


Figure 4: Biopsies of amyloid (A) AA 80% fibrillar, (B) AA 10% fibrillar.

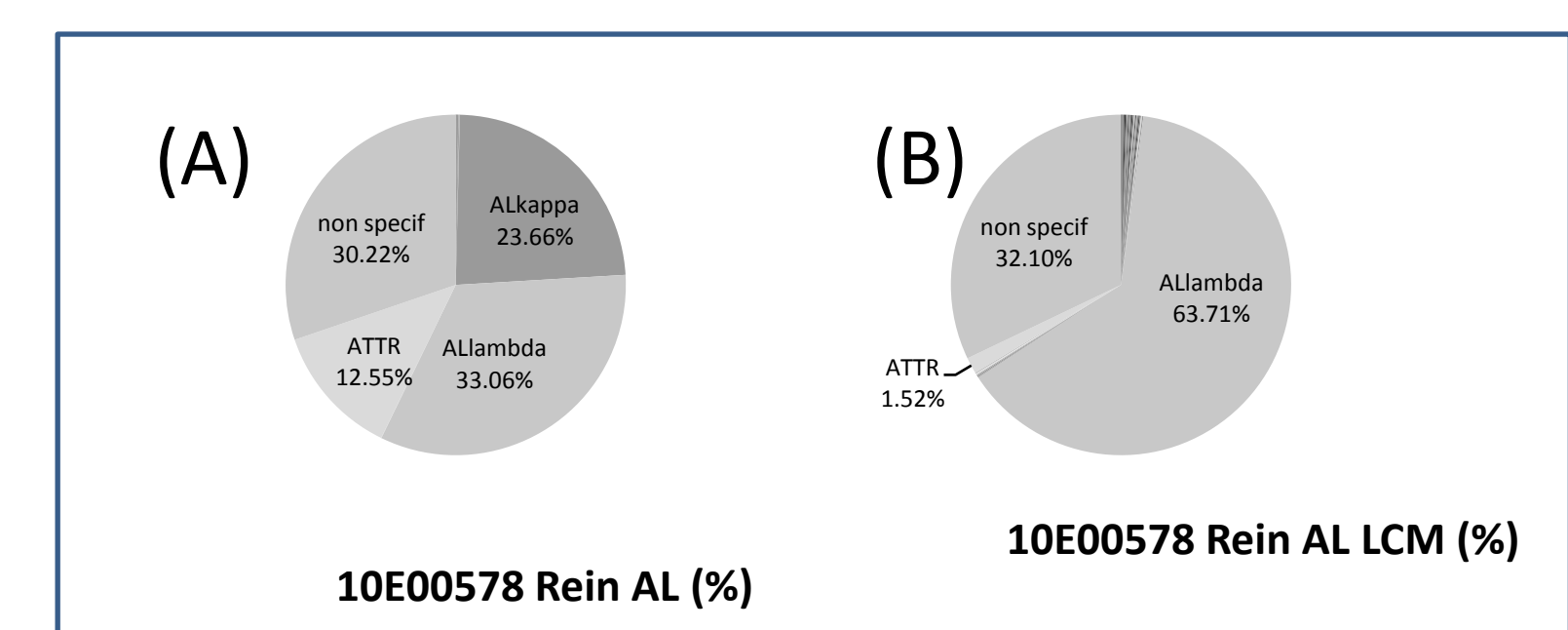


Figure 5: Biopsy of amyloid AL (A) raw tissue (50% , see Figure 2), (B) Laser Capture Microdissected LCM tissue (95%)

Accessory salivary glands (ASGB) Results.

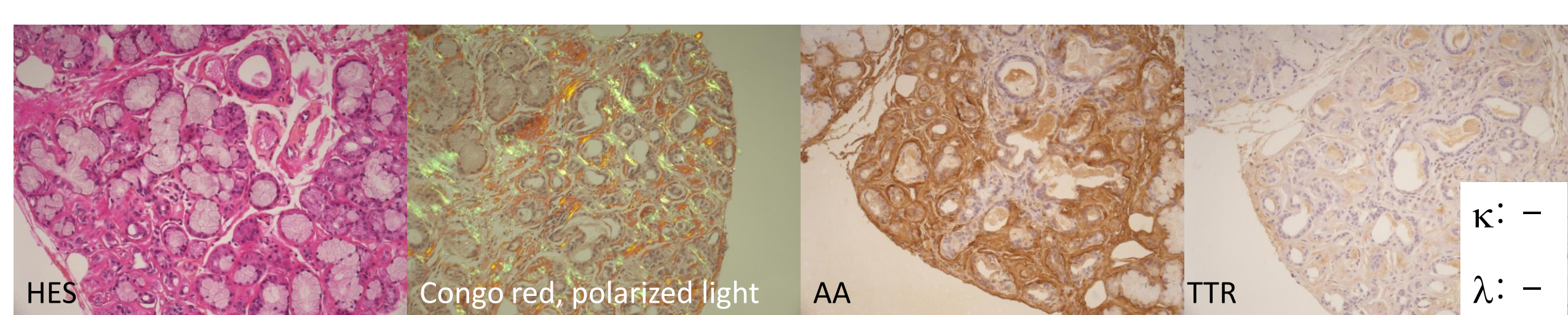


Figure 6: Anatomopathology studies of ASGB biopsies for AAL with (A) HE, (B) Congo red, (C) immunostaining AA, (D) immunostaining TTR. These biopsies were negative against Igκ and Igλ.

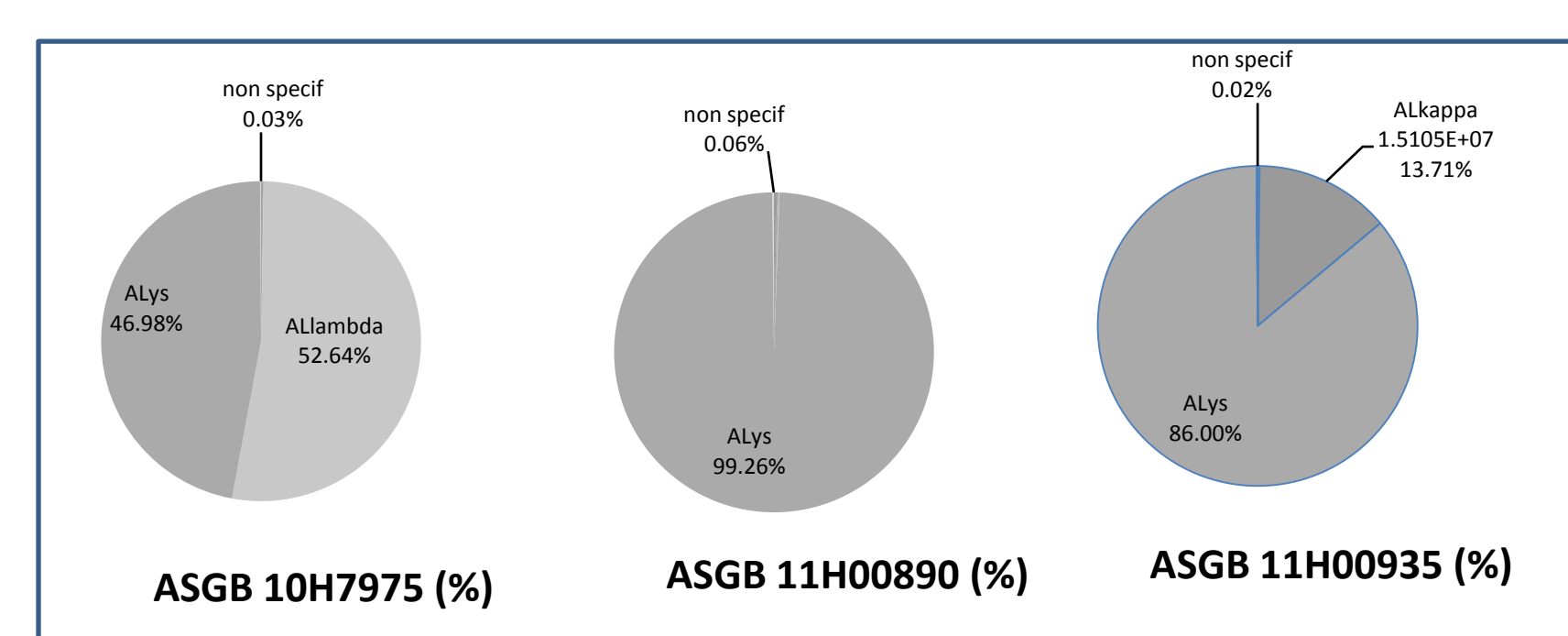


Figure 7: Biopsies of negative controls. ASGB is enriched in lysozyme, no SAMP or ApoE is present

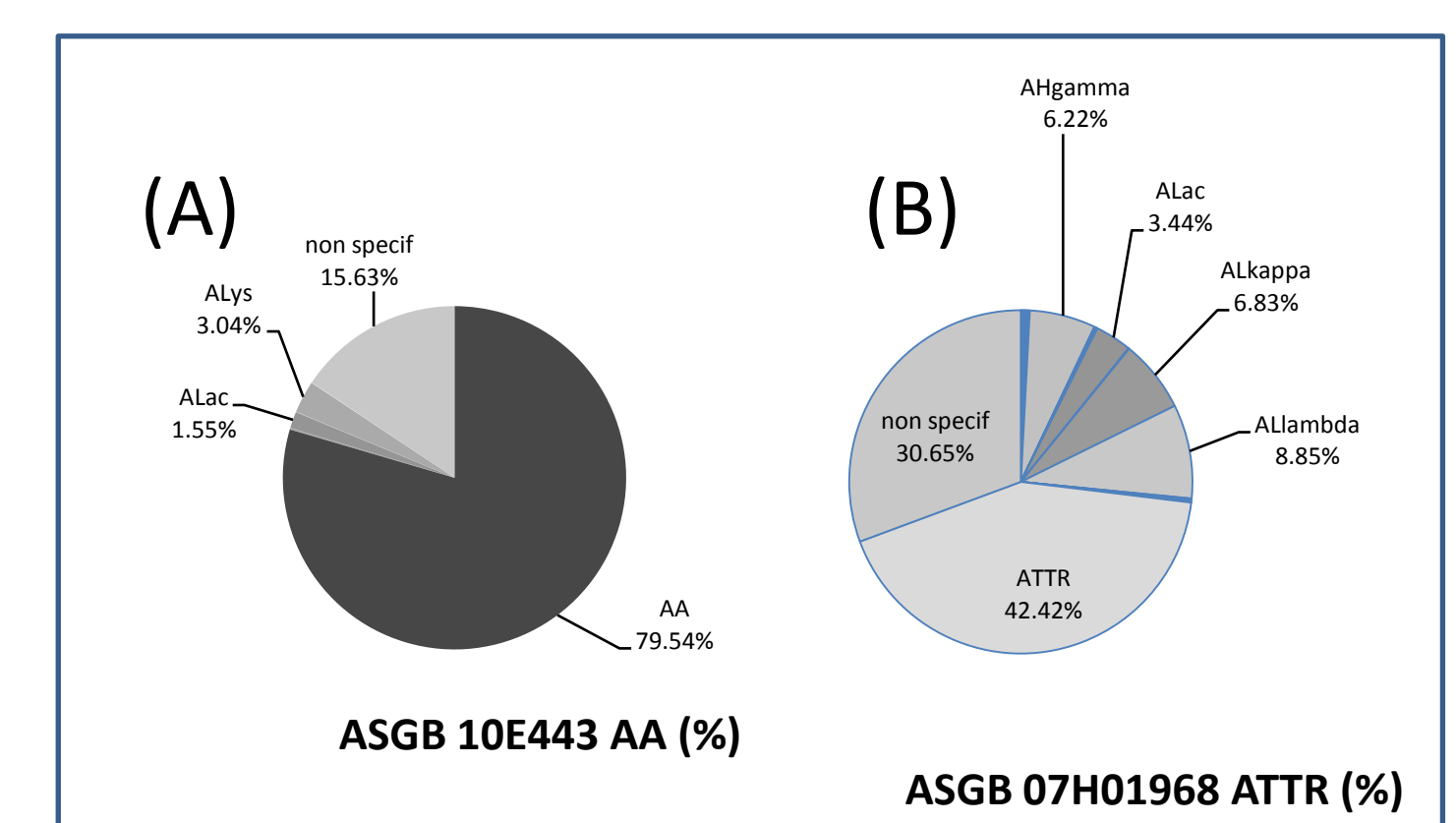


Figure 8: Biopsies of amyloid (A) AA, (B) ATTR.

ASGB are naturally enriched in Lysozyme C (from saliva). However in the control samples no SAMP and ApoE (amyloid deposits) could be seen. All the biopsies were assayed against the 20 major amyloid antibodies. For the two biopsies in Figures 6 and 8, the results were negative for ALκ and ALλ, and were positive for (A) AA and (B) ATTR respectively, using both techniques. ApoE and SAMP were also detected unambiguously among the major compounds (Figures 8 A and B).

Conclusion & Perspectives.

This strategy opens the way for a rapid and accurate amyloidosis subtyping directly from raw clinical samples and allows to avoid at the most the laser capture microdissection step which is highly time-consuming. This is of particular interest for classes that could not be distinguished by the classical histochemical analysis. Our next step will be to validate our approach to different amyloidoses and tissues with clinicians.

The whole analysis lasts 1 day for enzymatic treatment and roughly 10 slices are required and lasts 1 day for triplicate LC MS/MS and roughly 1 slice of 10µm is required. In order to increase cohorts for a realistic clinical application we intend to automatize the first step. Miniaturization is required to decrease sample consumption of the first treatment (only 10% of the sample is actually analyzed).

We want to characterize specifically the isoforms of protein involved. One example is ATTR addressed either by bottom-up (3) or top-down (4) strategies, where the transthyretin isoform can discriminate between senile systemic amyloidosis and familial transthyretin amyloidosis.

Acknowledgements

S. Liuu and E. Durighello received a grant from SAESPCI. This work was supported by CNRS, AP-HP Ville de Paris and the Association Française contre l'Amylose

References

1. S. Sethi, et al Clin. J. Am. Soc. Nephrol.,2010; 5(12): 2180-7.
2. L. Fernandez, et al JIOMICS, 2011, 1(1): 144-150.
3. J.S. Kingsbury, et al Anal. Chem. 2007, 79(5), 1990-8
4. R. Théberge, et al Int. J. Mass Spectrom. 2011; 300: 130-42
5. J.C. Silva, Mol Cell Prot, 2006, 5: 144-56